Sodium deficiency or aldosterone excess model		Aldosterone (pg/ml)
Diuresis	Furosemide + Chow	420.7 ± 96.1
	Furosemide + LSD	937.9 ± 60.0**
Sodium Deprivation	Chow	484.1 ± 74.2
	LSD	904.7 ± 44.8***
Osmotic Minipump	Vehicle	380.8 ± 63.9
	Aldosterone	1022.1 ± 192.6**

Table S1, related to Figure 1. Plasma aldosterone levels from sodium deficiency and chronic infusion studies.

Plasma aldosterone levels were measured by ELISA. Diuresis and sodium deprivation experiments had 6 mice/group, while osmotic pump experiments had 7-8 mice/group. Unpaired two-tailed t-test, $^{**}P < 0.01$, $^{***}P < 0.001$. Data are presented as mean ± SEM.

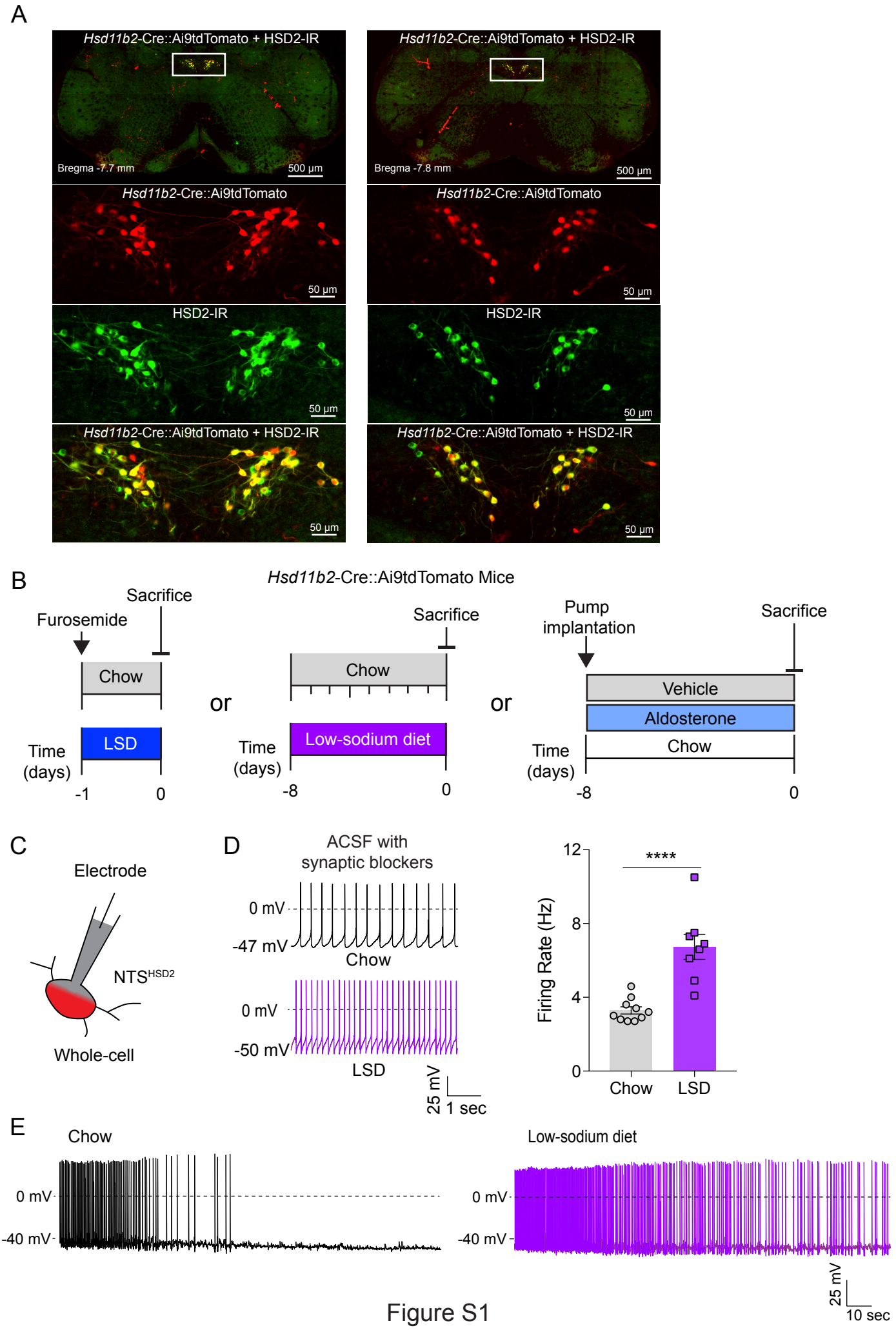
A
Hsd11b2-Cre::Ai9tdTomato + HSD2-IR
Bregma -7.7 mm
500 µm
Hsd11b2-Cre::Ai9tdTomato + HSD2-IR
Bregma -7.8 mm
500 µm
Hsd11b2-Cre::Ai9tdTomato
50 µm
HSD2-IR
50 µm
Hsd11b2-Cre::Ai9tdTomato + HSD2-IR
50 µm
B
Hsd11b2-Cre::Ai9tdTomato Mice
Sacrifice
Furosemide
Chow
LSD
Time (days)
-1
0
or
Sacrifice
Chow
Low-sodium diet
Time (days)
-8
0
or
Pump implantation
Sacrifice
Vehicle
Aldosterone
Chow
Time (days)
-8
0
C
Electrode
NTSHSD2
Whole-cell
D
ACSF with synaptic blockers
0 mV
-47 mV
Chow
0 mV
-50 mV
LSD
25 mV
1 sec
****
Firing Rate (Hz)
12
8
4
0
Chow
LSD
E
Chow
0 mV
-40 mV
Low-sodium diet
0 mV
-40 mV
25 mV
10 sec

Figure S1

Figure S1, related to Figure 1: Rundown of activity in whole-cell recordings of NTS^{HSD2} neurons.

All recordings were performed in the presence of synaptic blockers. Data are presented as mean ± SEM.

A) Validation of NTS tdTomato expression in *Hsd11b2*-Cre::Ai9tdTomato mice at two levels of the hindbrain. Top panels show low magnification images of *Hsd11b2*-Cre::Ai9tdTomato expression with HSD2 immunoreactivity (HSD2-IR). Below low magnification images are high magnification images of the NTS depicting *Hsd11b2*-Cre::Ai9tdTomato (top), HSD2-IR (middle), and *Hsd11b2*-Cre::Ai9tdTomato expression + HSD2-IR (bottom).

B) Schematics of experimental sodium deficiency and aldosterone infusion protocols. **C)** Schematic of whole-cell recordings.

D) Representative traces of whole-cell patch-clamp recordings immediately after breakthrough (left) and summary (right) of NTS^{HSD2} neuron activity from mice fed standard chow (Chow; top) or low sodium diet (LSD; bottom) for 8-12 days (Chow: n = 10 neurons from 3 mice; LSD: n = 8 neurons from 3 mice). Minimum and 0 mV membrane potentials are labeled in the representative traces for each treatment. Unpaired two-tailed t-test, ****$P < 0.0001$.

E) Representative long-term whole-cell recordings of NTS^{HSD2} neurons from Chow and LSD fed mice.

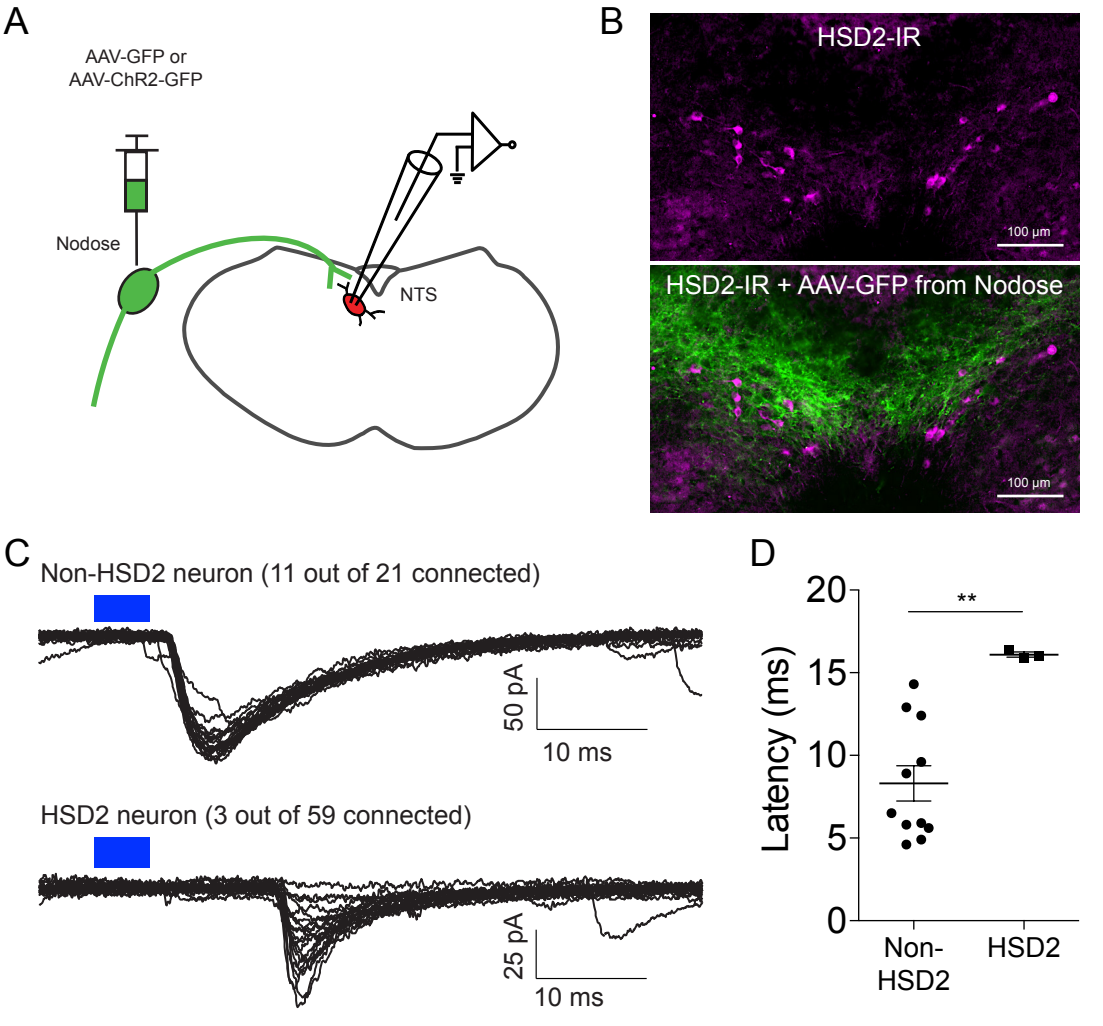
A
AAV-GFP or
AAV-ChR2-GFP
Nodose
NTS
B
HSD2-IR
100 µm
HSD2-IR + AAV-GFP from Nodose
100 µm
C
Non-HSD2 neuron (11 out of 21 connected)
50 pA
10 ms
HSD2 neuron (3 out of 59 connected)
25 pA
10 ms
D
Latency (ms)
20
15
10
5
0
**
Non-
HSD2
HSD2

Figure S2

Figure S2, related to Figure 1: ChR2-assisted circuit mapping of vagal afferent inputs to NTS^{HSD2} neurons.

Data are presented as mean ± SEM.

A) Schematic of AAV-GFP or AAV-ChR2-GFP nodose injections and experimental design for ChR2-assisted circuit mapping**.**

B) HSD2 immunoreactivity (HSD2-IR) in the NTS (top) and an overlay of vagal afferent fibers from AAV-GFP nodose injections (bottom).

C) Representative CRACM recordings from NTS Non-HSD2 (top) and HSD2 (bottom) neurons from *Hsd11b2-Cre*::Ai9tdTomato mice exhibiting light-evoked EPSCs (n = 4 mice). ChR2-expressing fibers around the recorded cell were photostimulated with blue light through the microscope objective.

D) Latency of light-evoked responses from NTS Non-HSD2 and HSD2 neurons. Unpaired two-tailed t-test, **P < 0.01.

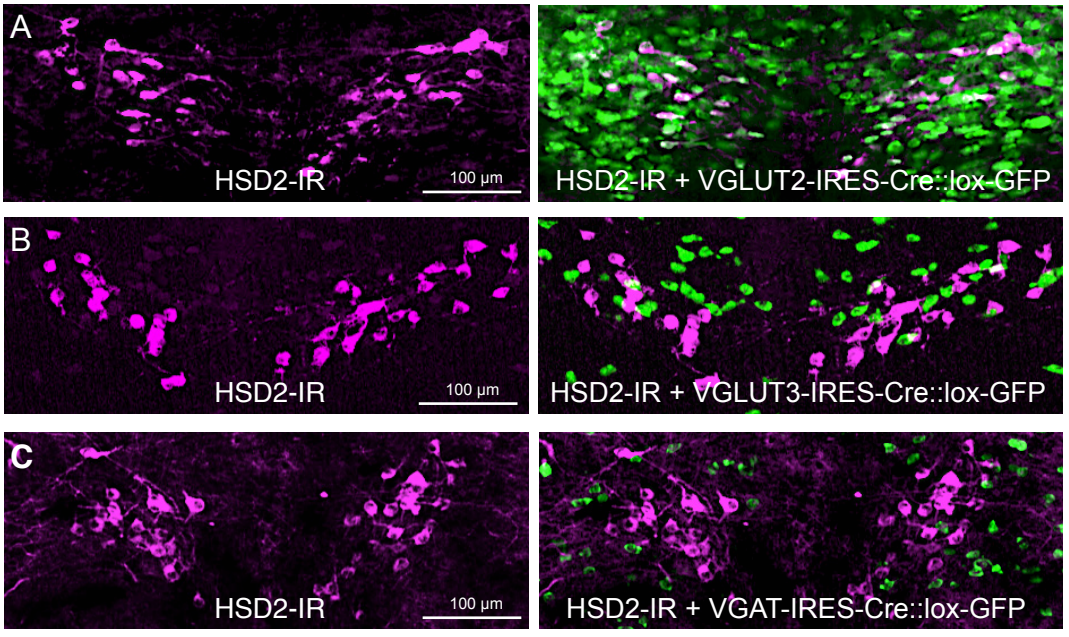
A
HSD2-IR
100 µm
HSD2-IR + VGLUT2-IRES-Cre::lox-GFP
B
HSD2-IR
100 µm
HSD2-IR + VGLUT3-IRES-Cre::lox-GFP
C
HSD2-IR
100 µm
HSD2-IR + VGAT-IRES-Cre::lox-GFP

Figure S3

Figure S3, related to Figure 2: NTS^{HSD2} neurons express VGLUT2.

NTS HSD2 immunoreactivity (HSD2-IR; all left panels) co-labeled with:

A) VGLUT2-IRES-Cre::lox-GFP reporter mouse expression.

B) VGLUT3-IRES-Cre::lox-GFP reporter mouse expression.

C) VGAT-IRES-Cre::lox-GFP reporter mouse expression.

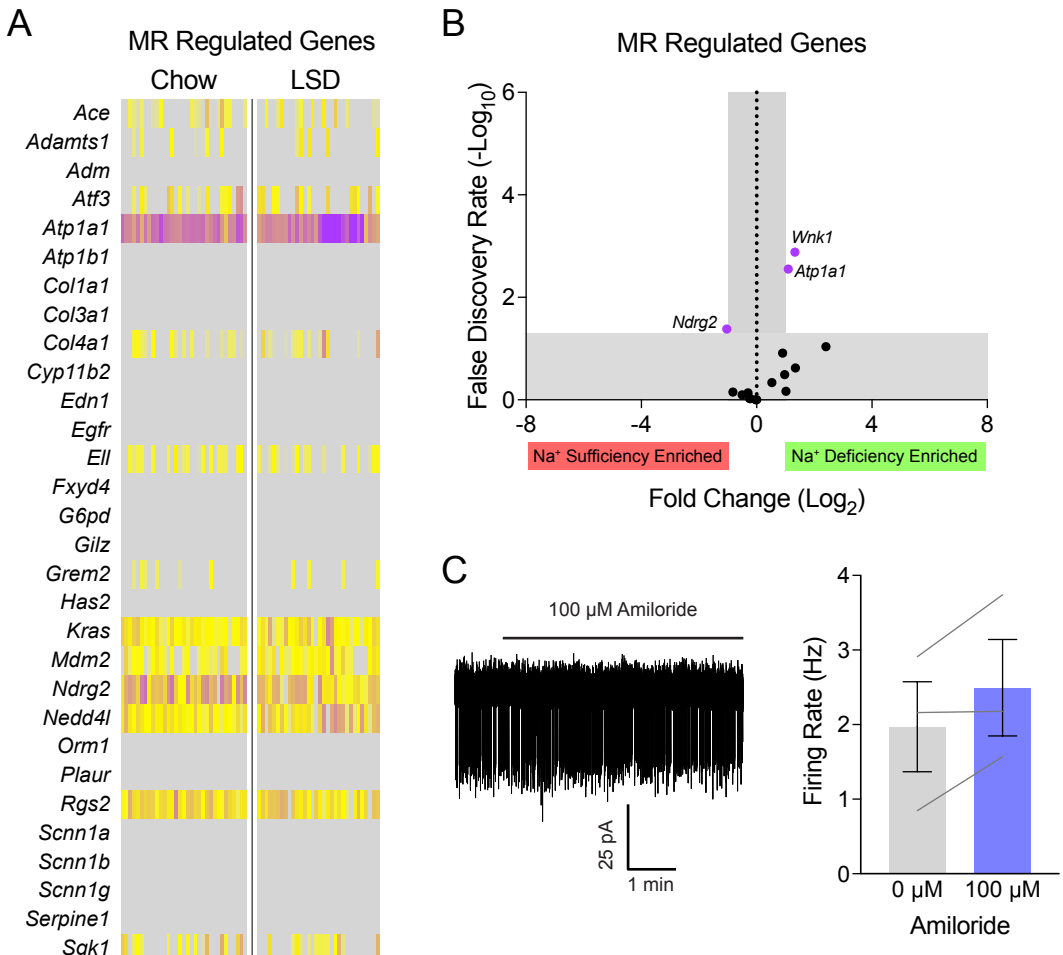
A
MR Regulated Genes
Chow
LSD
Ace
Adamts1
Adm
Atf3
Atp1a1
Atp1b1
Col1a1
Col3a1
Col4a1
Cyp11b2
Edn1
Egfr
Ell
Fxyd4
G6pd
Gilz
Grem2
Has2
Kras
Mdm2
Ndrg2
Nedd4l
Orm1
Plaur
Rgs2
Scnn1a
Scnn1b
Scnn1g
Serpine1
Sgk1
Slc12a3
Spp1
Tnxb
Ucp1
Ucp3
Usp2
Wnk1
0
6
≥12
Log2 CPM + 1
B
MR Regulated Genes
False Discovery Rate (-Log10)
6
4
2
0
-8
-4
0
4
8
Wnk1
Atp1a1
Ndrg2
Na+ Sufficiency Enriched
Na+ Deficiency Enriched
Fold Change (Log2)
C
100 μM Amiloride
25 pA
1 min
Firing Rate (Hz)
4
3
2
1
0
0 μM
100 μM
Amiloride

Figure S4

Figure S4, related to Figure 2: NTS^{HSD2} neuron RNA-Seq analysis of MR-regulated genes.

A) Heatmap showing single neuron expression patterns for MR-regulated genes (Viengchareun et al., 2007).

B) Volcano plot of MR-regulated genes affected by sodium deprivation. Dots outside the grey shaded region colored purple represent ion channel genes with significantly altered expression in response to sodium deprivation (Log_2 Fold Change > 1 or < -1, and False Discovery Rate < 0.05).

C) Representative cell-attached recording and summary of action potential firing rates of NTS^{HSD2} neurons from sodium-deprived mice before and after bath application of amiloride (n = 3 neurons from 2 mice). Data are presented as mean ± SEM.

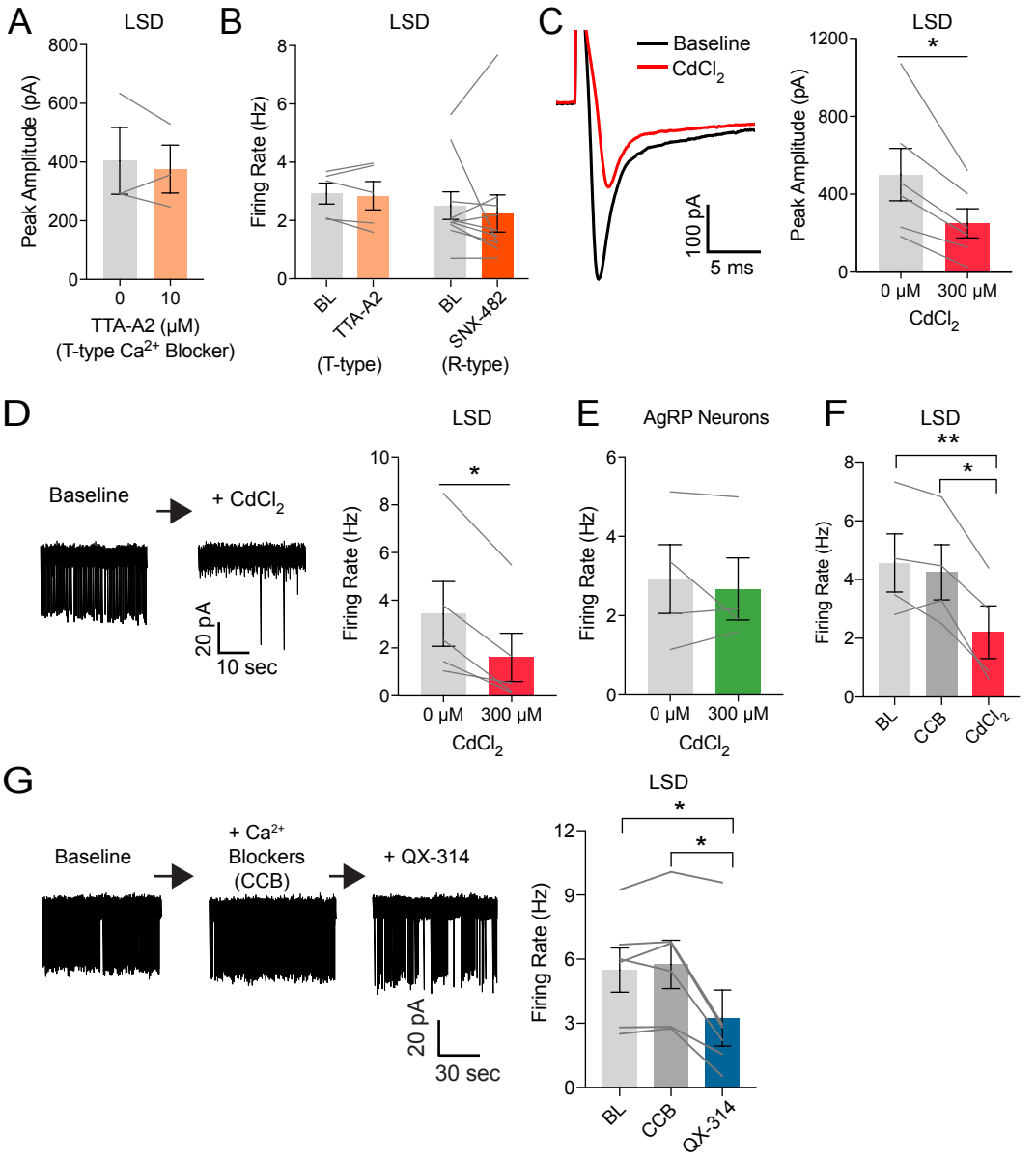
A
LSD
Peak Amplitude (pA)
800
600
400
200
0
0
10
TTA-A2 (μM)
(T-type Ca2+ Blocker)
B
LSD
Firing Rate (Hz)
8
6
4
2
0
BL
TTA-A2
BL
SNX-482
(T-type)
(R-type)
C
Baseline
CdCl2
100 pA
5 ms
LSD
*
Peak Amplitude (pA)
1200
800
400
0
0 μM
300 μM
CdCl2
D
Baseline
+ CdCl2
20 pA
10 sec
LSD
*
Firing Rate (Hz)
10
8
6
4
2
0
0 μM
300 μM
CdCl2
E
AgRP Neurons
Firing Rate (Hz)
6
4
2
0
0 μM
300 μM
CdCl2
F
LSD
**
*
Firing Rate (Hz)
8
6
4
2
0
BL
CCB
CdCl2
G
Baseline
+ Ca2+
Blockers
(CCB)
+ QX-314
20 pA
30 sec
LSD
*
*
Firing Rate (Hz)
12
9
6
3
0
BL
CCB
QX-314

Figure S5

Figure S5, related to Figure 4: State-dependent NTS^{HSD2} activity is mediated by TTX-resistant sodium channels but not T-type calcium channels.

All recordings were performed in the presence of synaptic blockers. Data are presented as mean ± SEM.

A) NTS^{HSD2} neuron peak evoked current amplitude from low sodium diet (LSD) fed mice before and after application of TTA-A2 (n = 3 neurons from 2 mice).

B) NTS^{HSD2} neuron action potential firing rates from low sodium diet (LSD) fed mice before (baseline; BL) and after application of TTA-A2 (10 μM; n = 5 neurons from 2 mice) or SNX-482 (300 nM; n = 10 neurons from 5 mice)**.**

C) Example traces (left) and summary (right) of peak evoked current amplitude before and after $CdCl_2$ treatment of NTS^{HSD2} neurons from LSD fed mice (n = 6 neurons from 3 mice). Paired two-tailed t-test, *P < 0.05.

D) Representative cell-attached recording (left) and summary (right) of action potential firing rates in NTS^{HSD2} neurons from LSD fed mice before and after $CdCl_2$ application (n = 5 neurons from 3 mice). Paired two-tailed t-test, *P < 0.05.

E) Action potential firing rates of hypothalamic AgRP neurons from fasted mice following $CdCl_2$ treatment (n = 4 neurons from 2 mice)**.**

F) Action potential firing rates of NTS^{HSD2} neurons from LSD fed mice at baseline (BL), after calcium channel blocker cocktail (CCB) treatment, and after $CdCl_2$ application (n = 4 neurons from 2 mice). Repeated measures ANOVA with posthoc analysis by Tukey's multiple comparisons test, *P < 0.05, **P < 0.01.

G) Representative cell-attached recording (left) and summary (right) of action potential firing rates of NTS^{HSD2} neurons from sodium-deprived mice at baseline (BL), after calcium channel blocker cocktail (CCB) treatment, and after QX-314 application (n = 6 neurons from 3 mice). Repeated measures ANOVA with posthoc analysis by Tukey's multiple comparisons test, *P < 0.05.

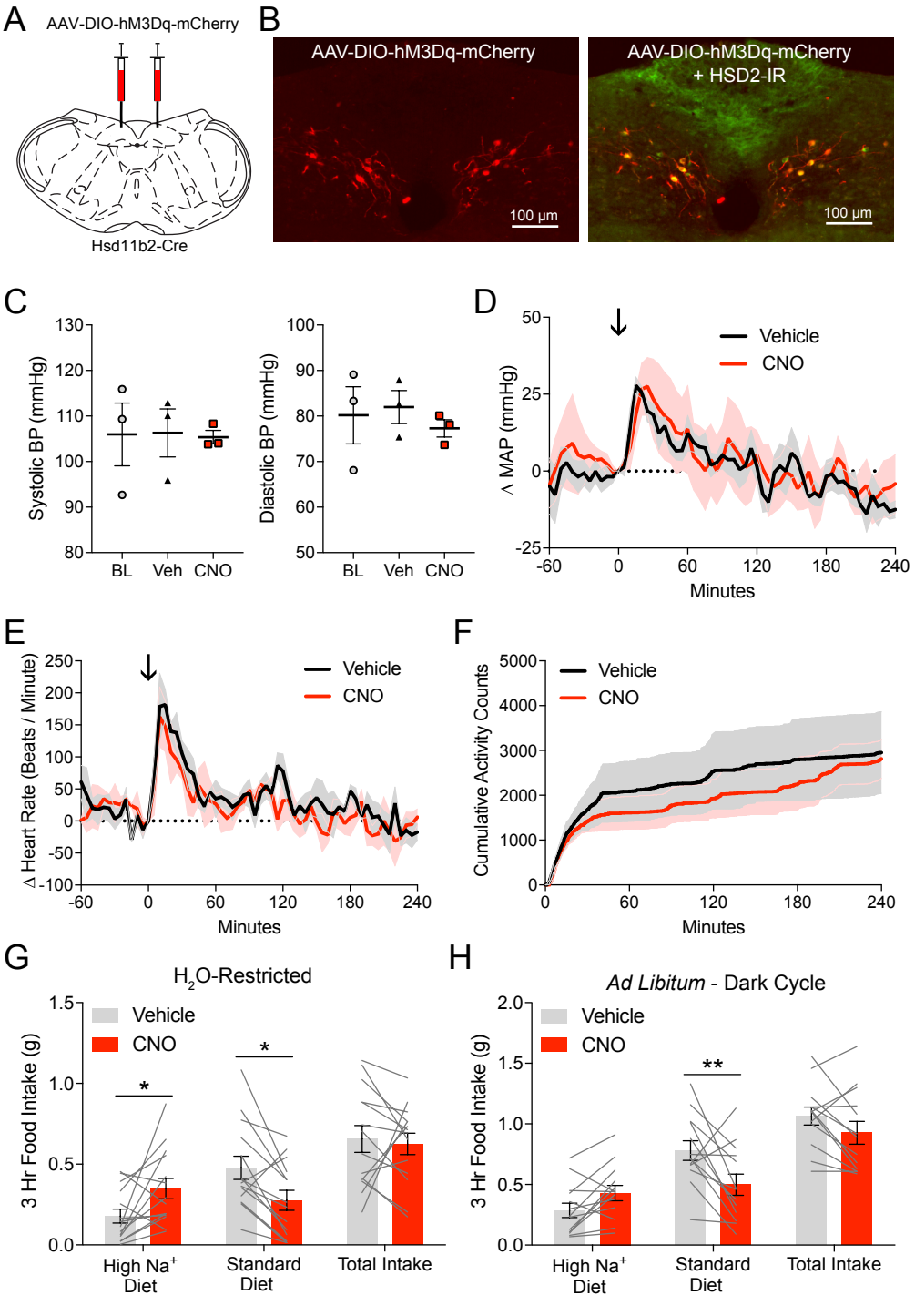
A
AAV-DIO-hM3Dq-mCherry
Hsd11b2-Cre
B
AAV-DIO-hM3Dq-mCherry
100 µm
AAV-DIO-hM3Dq-mCherry
+ HSD2-IR
100 µm
C
Systolic BP (mmHg)
Diastolic BP (mmHg)
BL
Veh
CNO
D
Vehicle
CNO
Δ MAP (mmHg)
Minutes
E
Vehicle
CNO
Δ Heart Rate (Beats / Minute)
Minutes
F
Vehicle
CNO
Cumulative Activity Counts
Minutes
G
H2O-Restricted
Vehicle
CNO
3 Hr Food Intake (g)
High Na+ Diet
Standard Diet
Total Intake
H
Ad Libitum - Dark Cycle
Vehicle
CNO
3 Hr Food Intake (g)
High Na+ Diet
Standard Diet
Total Intake

Figure S6

Figure S6, related to Figure 6: NTS^{HSD2} neuron activation affects food intake, but not cardiovascular function in euhydrated animals.

Data are presented as mean ± SEM.

A) Schematic of AAV-DIO-hM3Dq-mCherry injections.

B) Validation of hM3Dq expression in NTS^{HSD2} neurons from *Hsd11b2*-Cre mice (left) with HSD2 immunoreactivity (HSD2-IR; right).

C) Systolic blood pressure (left) and diastolic blood pressure (right) at baseline (BL), after vehicle injection (Veh), and following CNO/hM3Dq stimulation (CNO) of NTS^{HSD2} neurons in anesthetized animals (n = 3 mice).

D) Change in mean arterial pressure from telemetric recordings following chemogenetic stimulation of NTS^{HSD2} neurons. Arrow denotes ip injection of vehicle or CNO (n = 4 mice).

E) Change in heart rate from telemetric recordings following chemogenetic stimulation of NTS^{HSD2} neurons. Arrow denotes ip injection of vehicle or CNO (n = 3 mice).

F) Change in locomotor activity from telemetric recordings following chemogenetic stimulation of NTS^{HSD2} neurons (n = 4 mice).

G) Two-diet choice food intake of high sodium (High Na^+) diet and standard diet following CNO/hM3Dq stimulation of NTS^{HSD2} neurons in H_2O-restricted mice (n = 14 mice). Two-way repeated measures ANOVA followed by Sidak's multiple comparisons test, $*P < 0.05$.

H) Two-diet choice food intake of High Na^+ diet and standard diet following CNO/hM3Dq stimulation of NTS^{HSD2} neurons at the onset of the dark-cycle (n = 13 mice). Two-way repeated measures ANOVA followed by Sidak's multiple comparisons test, $**P < 0.01$.

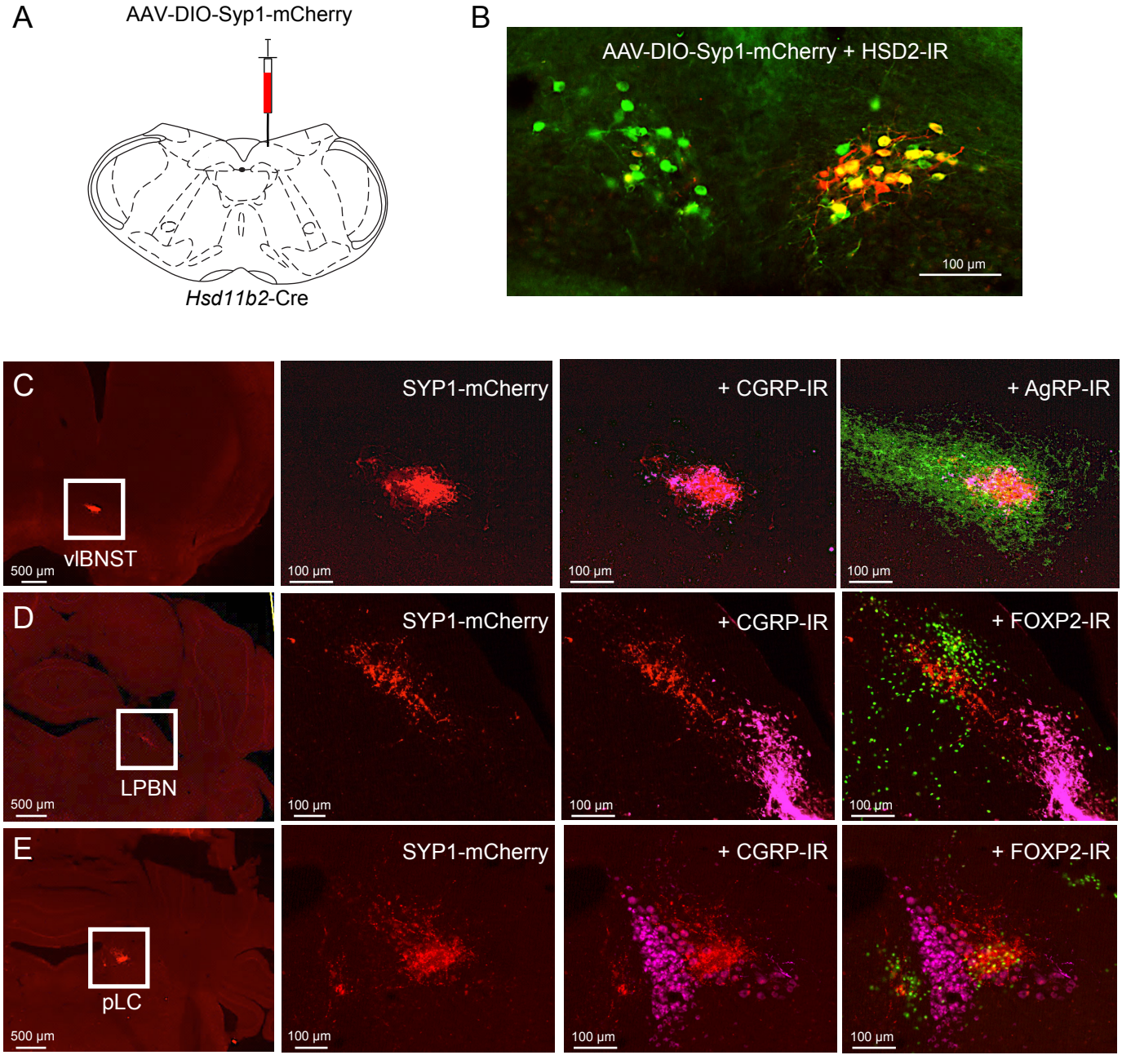
A
AAV-DIO-Syp1-mCherry
Hsd11b2-Cre
B
AAV-DIO-Syp1-mCherry + HSD2-IR
100 µm
C
vlBNST
500 µm
SYP1-mCherry
100 µm
+ CGRP-IR
100 µm
+ AgRP-IR
100 µm
D
LPBN
500 µm
SYP1-mCherry
100 µm
+ CGRP-IR
100 µm
+ FOXP2-IR
100 µm
E
pLC
500 µm
SYP1-mCherry
100 µm
+ CGRP-IR
100 µm
+ FOXP2-IR
100 µm

Figure S7

Figure S7, related to Figure 8: NTS^{HSD2} neuron projection mapping.

A) Schematic of AAV-DIO-Syp1-mCherry injections.

B) Validation of Syp1-mCherry expression in NTS^{HSD2} neurons from *Hsd11b2-Cre* mice with HSD2 immunoreactivity (HSD2-IR).

C) NTS^{HSD2} neuron projections to the vlBNST (left and middle-left). These projections overlap with both calcitonin gene-related peptide (CGRP)-IR (middle-right) and AgRP-IR (right).

D) NTS^{HSD2} neuron projections to the LPBN (left and middle-left). These projections avoid the CGRP-IR field (middle-right), but do overlap with FOXP2-IR (right).

E) NTS^{HSD2} neuron projections to the pLC (left and middle-left). These projections avoid the locus coeruleus labeled by CGRP-IR (middle-right), but overlap with FOXP2-IR (right) in this region.